Optimal Coordination of VSC-Interfaced Subsystems to Safeguard the Frequency Performance of Cyber-Physical Power Systems

Giannakopoulos, Georgios; Guerra, Arcadio Perilla; Torres, José Luis Rueda; Palensky, Peter

DOI
10.1002/9781394191529.ch28

Publication date
2025

Document Version
Accepted author manuscript

Published in
Smart Cyber-Physical Power Systems

Citation (APA)
Giannakopoulos, G., Guerra, A. P., Torres, J. L. R., & Palensky, P. (2025). Optimal Coordination of VSC-Interfaced Subsystems to Safeguard the Frequency Performance of Cyber-Physical Power Systems. In *Smart Cyber-Physical Power Systems: Fundamental Concepts, Challenges, and Solutions* (Vol. 1, pp. 715-726). Wiley. https://doi.org/10.1002/9781394191529.ch28

Optimal coordination of VSC-interfaced subsystems to safeguard the frequency performance of cyber-physical power systems

Georgios Giannakopoulos, Arcadio Perilla Guerra, José Luis Rueda Torres*, Peter Palensky

Intelligent Electrical Power Grids, Department of Electrical Sustainable Energy, Faculty of Electrical Engineering, Mathematics and Computer Science, Delft University of Technology, The Netherlands
* Corresponding author: j.l.ruedatorres@tudelft.nl

1. Motivation and Scope of the Chapter

Integrated energy systems are increasingly dominated by the operation and control of power electronic interfaced (PEI) devices at generation, multi-energy storage, transmission, and distribution, and responsive demand [1], [2]. Simultaneously, the so-called, voltage source converter technology (VSC), is positioning as the preferred option for implementation of PEI due to its versatile and flexible operation and control modes [1], [3]. The progressive phase-out of conventional alternating current technologies (e.g. synchronous generators), and their replacement by VSC-based PEI brings major changes in the dynamic behavior of the emerging forms of DC-AC system topologies [4]. For instance, reduced, limited, or absent control capabilities may entail unprecedented frequency or voltage deviations, which could happen in shorter time scales (e.g. less than a fraction of a second), when compared to typical deviations observed in conventional systems dominated by synchronous generators [4], [5]. This motivates a renewed emphasis and significant research efforts towards the development of models of multi-area and multi-energy HVDC-HVAC cyber-physical power system, which enable a trustworthy computer-aided investigation of new forms of dynamic stability phenomena [4], [6].

This chapter particularly focuses on the problem of the implications of altered active power balance on the dynamic frequency performance of cyber-physical power systems. To this aim, and, in line with the current state-of-the-art, it is considered that the PEIs of new component additions may be equipped with emerging method(s) for fast frequency support (FFS) as a function of the underlying operation and control capabilities of the latest VSC technologies [7]. Hence, FFS is assumed as an available functionality of new key components like turbines (WTs)[8], solar-photovoltaic systems (PVs)[9], HVDC links [10] and power-to-gas conversion units (e.g. electrolysers) [11].

FFS working under the control principle of active power gradient is one of the promising options of effective mitigation of undesirable fast and significant dynamic frequency deviations [12]. This technique can be tuned for one or several disturbances affecting the active power balance. This can be done by considering two settings, i.e. the amount of active power (ΔP) to be quickly injected/absorbed, and the rate or gradient (APG) at which the active power is adjusted. Due to the different dynamic properties of PEI distributed across a multi-area and multi-energy HVDC-HVAC cyber-physical power system, achieving an optimally effective FFS constitutes an open research challenge [12][13]. For instance, the investigation discussed in [12] illustrates the limited effectiveness of uncoordinated tuning, taking as an example the challenges of calibrating the active power gradient based FFS applied to two-terminal VSC-based HVDC interconnector.

The risk of ineffective FFS is specially higher in systems with low headroom and adverse interplay of the resources guided by FFS under different forms of active power imbalances[13]. Recently, attempts to tune FFS is systems with few selected PEIs have been conducted based on single parameter parametric sensitivities. Nevertheless, as shown in [13] and [14], optimal effectiveness under diverse operating conditions and disturbances is not ensured.

Hence, proposing a suitable optimization oriented problem statement is also challenge tackled in this chapter. The goal is to obtain an effective coordinated tuning of PEIs. To this end, and for illustrative purposes, the proposed multi-area and multi-energy HVDC-HVAC cyber-physical power system assumes FFS attached to VSC-HVDC links interconnecting the synchronous areas of the system as well as attached to proton exchange membrane (PEM) electrolysers. The example shown in the chapter considers the occurrence of a large-size active power imbalance.

The proposed optimization statement targets the enhancement of the overall frequency stability by properly and cooperatively mitigating the imbalance through controllable active power resources that are in service in the synchronous areas, also taking into account their own characteristics and limitations for FFS. The model is implemented by using library components of the software package known as DIgSILENT PowerFactory 2022 (DPF2022), whereas the optimization search process of the mean-variance mapping optimization (MVMO) algorithm, described in [15] is tailored and deployed in the chapter to find a near-to-optimal solution within a restricted computational budget (due to the need of repetitively performing RMS simulations.

The reminder of the chapter is structured in the following sequence: The multi-area and multi-energy HVDC-HVAC cyber-physical power system is presented in Section 2. The proposed optimization problem statement is provided in Section 3. Section

4 concisely overviews the application of the MVMO algorithm. Findings from numerical simulations are given in Section 5. Concluding reflections and prospective future subsequent research aspects are summarized in Section 6.

2. THE HVDC-HVAC CYBER-PHYSICAL TEST POWER SYSTEM

The first version of the PST16 power system is presented in [15]. This system is modified and utilized in this chapter for the purpose of testing the proposed optimization statement on a futuristic multi-area and multi-energy HVDC-HVAC cyber-physical system. This entails using the model to perform the diverse RMS simulations of interest when tackling the challenging optimization search process. The topological layout of the multi-area and multi-energy HVDC-HVAC cyber-physical system is shown in Fig.1. It is worth pointing out that the weak HVAC tie-lines in the original system are replaced with three VSC-based HVDC links in different areas. Taking into account the forecasted hydrogen demand scenario shown in [16], 30% load demand of each area is replaced with eleven PEM electrolyzers. This essentially done to investigate the importance and possible collateral impacts of the considered installation location with respect to disturbance altering the active power balance and overall dynamic frequency performance of the system. In this way, the proposed system basically allows investigating the effectiveness of an assumed form of FFS to be attached to the considered controllable active power sources, like the VSC-HVDC inter-area links and the PEM electrolysers. Additional details about adopted component models and the parameters used in the multi-area and multi-energy HVDC-HVAC cyber-physical system are available in [17].

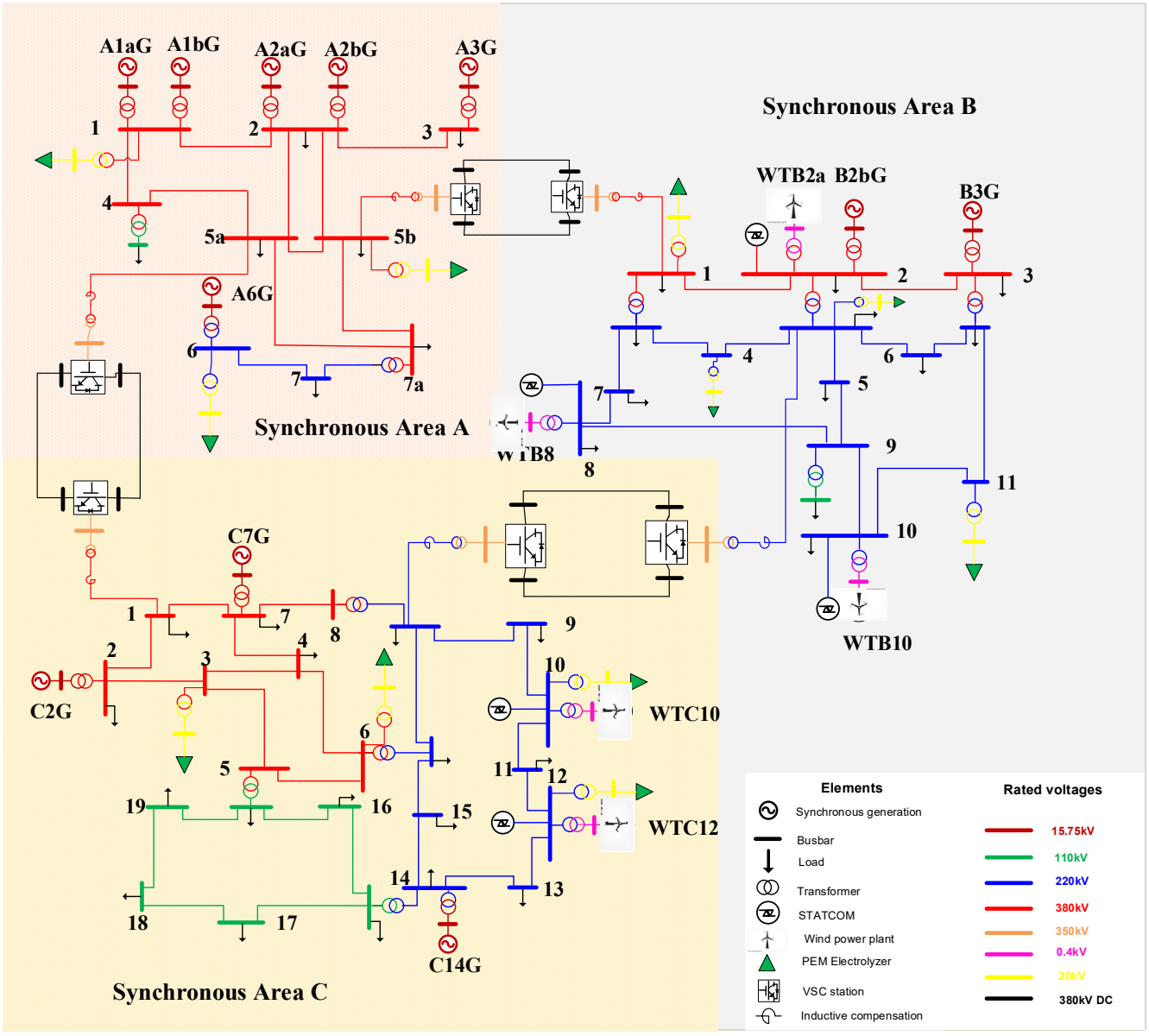

Fig. 1. Single-line diagram of the proposed futuristic multi-area and multi-energy HVDC-HVAC cyber-physical system.

A model provided by DIgSILENT which is detailed in [17] and developed under the guidelines outlined in [18], is utilized for modelling the steady-state and dynamic performances of the VSC-HVDC inter-area links in DPF2022. The model comprises

of two converter stations which exploit the current-vector control strategy proposed in [19]. On the DC side, the converters are configured in a bi-polar layout and on the AC side, they are connected to the corresponding local synchronous area through conventional three winding power transformers. Specific active and reactive power setpoints are provided to the HVDC links for recreating the power flow profiles of the AC tie lines that were used in the original PST16 system. These setpoints are used by the inverter stations to control the power output. The rectifiers operate based on the DC voltage and reactive power references and are responsible of maintaining the active power balance. Fig. 2 shows the modified P/Vdc controller of the links, which enables FFS from the HVDC links. Basically, the APG control loop is introduced which controls the amount of power (ΔP) and the active power (APG) injection rate when a systemic frequency deviation is detected. As envisioned in this chapter, the parameter selection is determined based on the solution to a formally defined optimization problem. This is done by using the proposed formulation, which considers the time evolution of the dynamic frequency responses of each synchronous area considered in the optimization of the FFS attached to the involved controllable resources for active power support. This aspect is elaborated in Section 3. It is assumed that the VSC-HVDC links can adjust their power flows for FFS, once in each simulation, with an activation delay of approximately 0.3 s after the occurrence of a disturbance altering the overall active power balance.

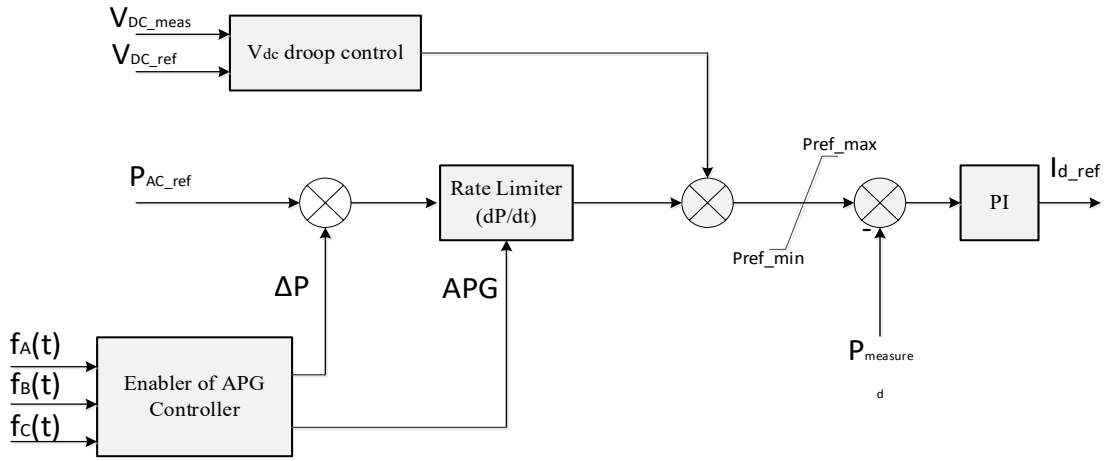

Fig. 2. Structure of the proposed modification for P/Vdc controller attached to the VSC-HVDC inter-area links.

In this chapter, the modelling of PEM electrolysers has been done considering them as electromagnetically decoupled general loads, which are interconnected to the local grid through conventional power transformers. This assumption is motivated by a similar modelling approach reported in [20]. The electrolysers are activated for FFS and their consumption is dynamically controlled in proportion to the measured systemic frequency deviation. The overall control structure considered in this chapter for the PEM electrolyzers is shown in Fig. 3. The available bid and the ramp rate determines the tuning of the proposed frequency controller. The APG control block presented in Fig. 3 is used for the dynamic active power adjustment. It operates as per the solution of the optimization problem under the proposed formulation, which is explained in detail in Section 3. The alternative representation of PEM electrolyzers, as discussed in [20], offers a versatile, yet trustworthy model for numerical simulation based power system stability assessments. This representation has a primary focus on the critical parameter of interest, which is the ramp-rate of the electrolyser's active power consumption.

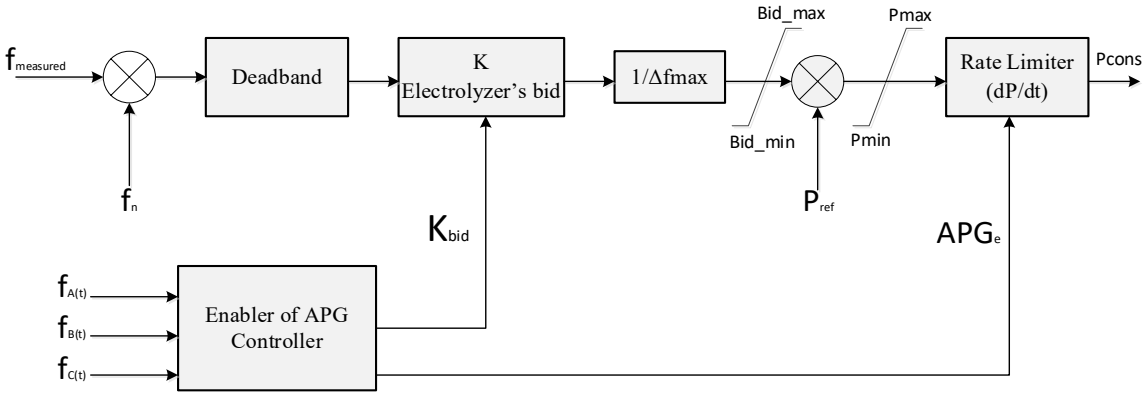

Fig. 3. Proposed frequency controller for PEM electrolysers.

3. STATEMENT OF THE OPTIMIZATION OF FFC FOR PEI

A system with multiple synchronous areas that are electromagnetically decoupled through VSC-HVDC inter-area links entails a particular characteristic of the dynamic frequency response for each individual area. Hence, any active power imbalance occurring in one of the synchronous areas shall be in principle confined within the affected area [21]. In other terms, without the intervention of the VSC-HVDC inter-area links, the frequencies of the other areas remain constant at their corresponding nominal values. The VSC-HVDC inter-area links can, however, be controlled to dynamically alter the inter-area power exchange to

provide FFS to the affected area. In such a case, the supporting synchronous area undergoes a deviation of frequency from the nominal value as a function of the defined form of controlled variation of the power exchange between the involved synchronous areas.

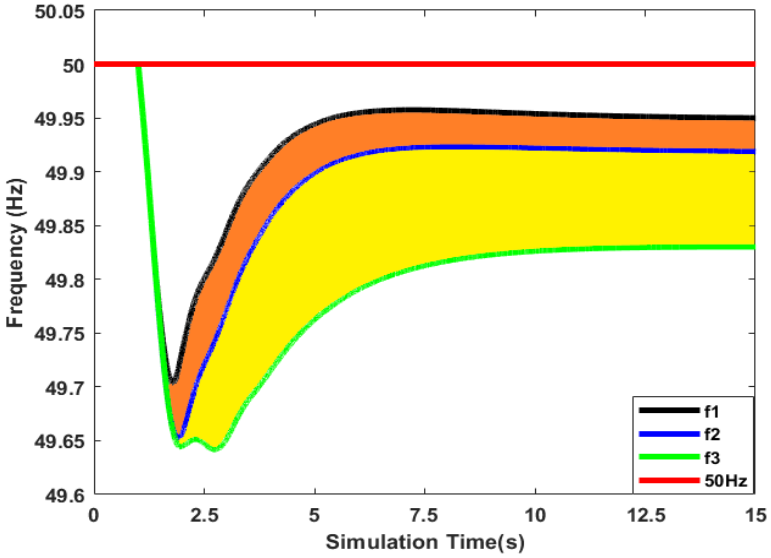

Fig. 4. Example visualization of the optimal tuning of FFC.

The representation in Fig. 4 conveys that the objective function (OF) of the proposed problem statement is conceived to minimize the graphical area in the three-area multi-energy HVDC-HVAC cyber-physical system. The minimization is done among each pair of the frequency responses, of the synchronous areas that are participating in the frequency regulation. In this manner, the problem statement attempts to share the active power imbalance among the areas as per the kinetic energy characteristics and active power reserves. Therefore, it results in the improvement of the frequency response of the affected synchronous area, with very little impact on the supporting synchronous areas. The scheme tries to develop an artificially coupled frequency response, securing the best possible response for the complete system, in a decoupled multi-area HVDC-HVAC cyber-physical system. This is done by optimally dividing the imbalance across the active power reserves available for each area. The mathematical representation of the problem formulation is shown in (1)-(7).

Minimize:

$$OF(\mathbf{x})=\int_0^{\tau}[|f_A(\mathbf{x},t)-f_B(\mathbf{x},t)| + |f_B(\mathbf{x},t)-f_C(\mathbf{x},t)|+|f_A(x,t)-f_C(x,t)|]dt \quad (1)$$

subjected to: $$\mathbf{x_{min}}\leq\mathbf{x}\leq\mathbf{x_{max}} \quad (2)$$

where $f_k(\mathbf{x},t)$ is the instantaneously measured frequency in the k-th area at instant t, on application of the candidate solution $\mathbf{x}$. Two variables are present in the optimization vector $\mathbf{x}$ for each of the FFS elements that take part in the fast frequency regulation. In the multi-area and multi-energy HVDC-HVAC cyber-physical system, three VSC-HVDC inter-area links and eleven electrolyzers have been integrated. Thus, $\mathbf{x}$ constitutes of a total of 28 optimization variables $\mathbf{x}$.

The first parameter for the VSC-HVDC inter-area links indicates the APG ramp rate. The second parameter reflects the corresponding link's ΔP. The PEM electrolyzers are characterized by two primary parameters: the first one represents the electrolyser's bid size (Bid_e), while the second parameter signifies the rate of change in the electrolyser's consumption (APG_e). In (3), the optimization vector $\mathbf{x}$ is observed. Additionally, each optimization variable is subject to specific bound constraints based on the technical limitations of each unit. For the VSC-HVDC inter-area links, the new setpoint should not exceed the rated capacity of the link in both directions [13], [14], and the ramp rate should not surpass the maximum rate that the link can handle [22]. Likewise, for the PEM electrolyzers, the available bid must not exceed 70% of their rated capacity, and the ramp rate should not exceed 0.5 pu/s, as elaborated in the references [23], [24], and [25]. The assumed boundary conditions for these optimization variables are specified in (4)-(7).

$$\mathbf{x}=\begin{bmatrix}\Delta P_{HVDC_1},APG_{HVDC_1},\ldots,\Delta P_{HVDC_i},APG_{HVDC_i},K_{ebid_1},\\ APG_{e_1},\ldots,K_{ebid_j},APG_{e_j}\end{bmatrix} \quad (3)$$

$$P_{refi}+\Delta P_i\leq|P_{rated_i}| \quad (4)$$

$$0\frac{GW}{min}\leq APGi\leq 60\frac{GW}{min} \quad (5)$$

$$0\leq K_{bid_w}\leq 0.7P_{elec_{rate_w}} \quad (6)$$

$$0\leq APG_{e_w}\leq 0.5\ P_{elec_{rated_w}}\ \frac{MW}{s} \quad (7)$$

4. Solution by Mean-Variance Optimization

A powerful metaheuristic solver, known as the mean-variance mapping optimization (MVMO) algorithm, has been utilized in this chapter for solving the optimization problem. The algorithm has displayed significant potential in the solution of computationally heavy problems related to power systems, including diverse statements of optimal power flow, and parametric identification of power system dynamic equivalents [26]. The flowchart of the MVMO algorithm is schematically depicted in Fig. 5.

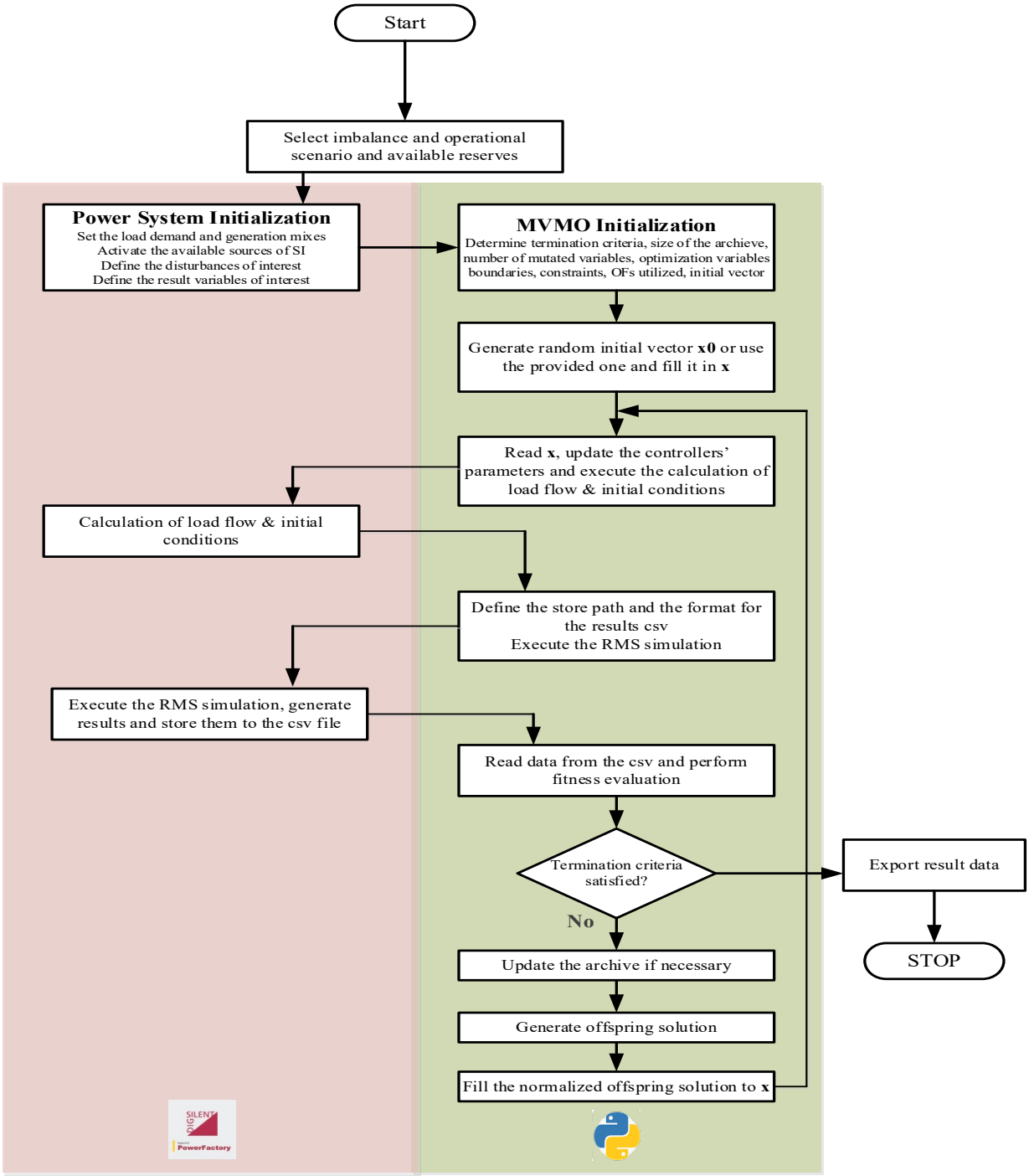

Fig. 5. Solution procedure performed by MVMO.

Initially , the algorithm computes a random initial vector, which is within the research space that is defined by the boundary conditions assumed for each variable. The selected parameters are then applied to the corresponding system element in DPF2022 and an RMS simulation is performed for obtaining the time evolution of the dynamic frequency responses that are of interest for evaluating the systemic frequency performance. The latter ones are exploited to execute the fitness evaluation and calculation of the OF value. Numerous predefined fitness evaluations follow the same process. In this chapter, assuming a restricted computing budget due to time consuming RMS simulations, 100 pre-defined fitness evaluations are considered, which act as the algorithm termination criterion. During these evaluation, MVMO generates potential offspring solution vectors based on the optimization variables of the best-performing parent solution achieved thus far. These offspring solutions are generated in accordance with evolution guidelines established by a mapping function for each variable. These guidelines take into consideration statistical data, including the mean and variance of each optimization variable as inputs. As a result, the most successful parent solutions and the statistical data pertaining to each variable are recorded in an archive of a predefined memory capacity. Eventually, once the termination criterion has been met, the solution vector contains the variables that have minimized the OF, resulting in the optimal frequency response for the system within the specified number of fitness evaluations. The algorithm operates within a normalized range of [0,1] for each variable, thereby eliminating the need for subsequent penalties or corrections. More comprehensive information regarding the MVMO algorithm and its calibration can be found in [26].

5. Simulation Analysis

For assessing the performance of the proposed statement for tuning the FFC attached to the considered VSC-HVDC inter-area links and PEM electrolysers, a scenario is considered involving a significant and frequently occurring active power imbalance within the multi-area and multi-energy HVDC-HVAC cyber-physical system. This scenario involves the sudden loss of the largest synchronous generator unit based power plant (SGU A1a) in the synchronous area with the lowest inertia conditions, referred to as area A. This event is initiated at the beginning of the simulation, within the first second, and, in response to the disturbance, all the PEI elements installed across the different areas are activated for providing FFS.

Under a condition where no FFS is provided from any PEI element, the SGUs present in the affected synchronous area are the only elements that can support the primary frequency control. In such a condition, the frequency of the synchronous area A reduces rapidly with a rate of -0.51Hz/s up to 48.8Hz. Subsequently, the frequency starts to recover and eventually, after about 15s, it settles at 49.55 Hz. The HVDC links isolate this affected area from the rest of the system. Therefore, the frequencies in the synchronous areas B and C are undisturbed and they are not subjected to any change in their power flow exchanges. This can be seen in the dashed line in Fig. 6. The affected area frequency response defy the acceptable limits, which are set by transmission system operators (TSOs) in [27], and this clearly shows the requirement of FFS from PEI units.

In case the PEI elements are operated to deliver FFS, the proposed problem statememt can be effectively utilized for their FFC parameter tuning. Once the termination criterion is fulfilled, the solution vector **x** takes the form as presented in (8). The corresponding frequency response of the system is shown in Fig. 6. It is observed that the affected synchronous area frequency considerably improves on sharing the imbalance among the available supporting synchronous areas. The initial rate-of-change of frequency (RoCoF) drops to -0.30 Hz/s from -0.51 Hz/s. This is solely because of the quick response from the PEM electrolyzers present in the affected synchronous area. Subsequently, the synchronous area A frequency decreases to 49.76 Hz and it settles at 49.93Hz within a time duration of 5 s. The frequencies in the synchronous areas B and C fall to 49.92Hz and 49.93Hz, respectively, and they eventually stabilize at 49.93Hz and 49.94Hz, respectively. This operation validates the objective of the proposed statement, which is to minimize the frequency drop in the affected area, while also minimizing the impact on the active power supporting areas through appropriate tuning of FFC. As such, the formulation aims to establish uniform frequency responses across all interconnected synchronous areas, by effectively utilizing the available active power reserves, thus resulting in frequency responses that fall within the acceptable operating limits as defined by TSOs in [27].

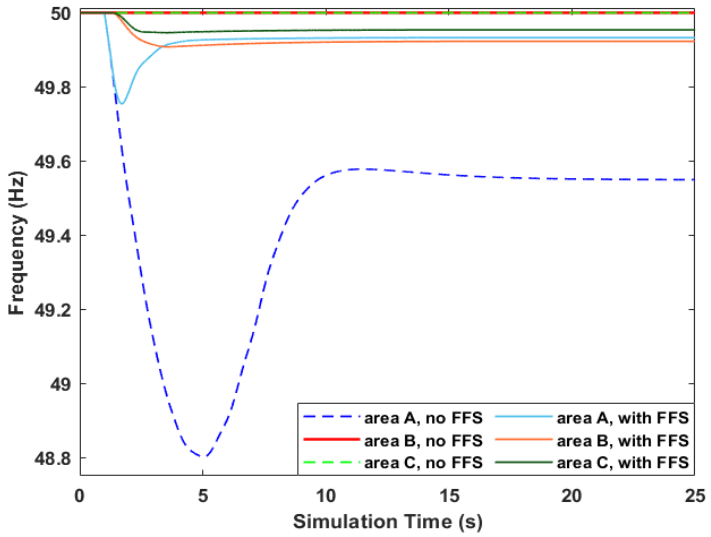

Fig. 6. Dynamic frequecny evolution of the synchronous areas, with and without FFS.

x=[932,-185,796,-377,412,-188.9,95.4,67.5,38.7,72.2,21.4,62.3,242,121,85.6,29.2,186,36.7,12.1,16.4,166,74.5,32.9,

24.7,45.9,94.5,118,53.5] (8)

Equation (8) also denotes that the electrolyzers play a considerably important role for the FFS. On the occurrence of an imbalance, the PEM electrolyzers present in synchronous area A are activated to offer rapid support and arrest the initial drop, before the VSC-HVDC inter-area links are activated. The VSC-HVDC inter-area links A-B and A-C start changing their powers after 0.3 s. The power delivered to areas B and C are reduced such that support can be provided to the affected areas. On the other hand, the VSC-HVDC inter-area link B-C alters its power flow direction for balancing the impact on the synchronous areas B and C. In this manner, the optimization problem statement is able to achieve an optimal share of power among the affected synchronous areas as per their kinetic energy characteristics and active power reserves. The PEM electrolysers present in areas B and C are also activated for the purpose of FFS and mitigating the influence on the supporting areas, which lead to comparable post-disturbance frequency responses. Consequently, the formulation strives to achieve a coordinated frequency response within a multi-area system that is electromagnetically decoupled.

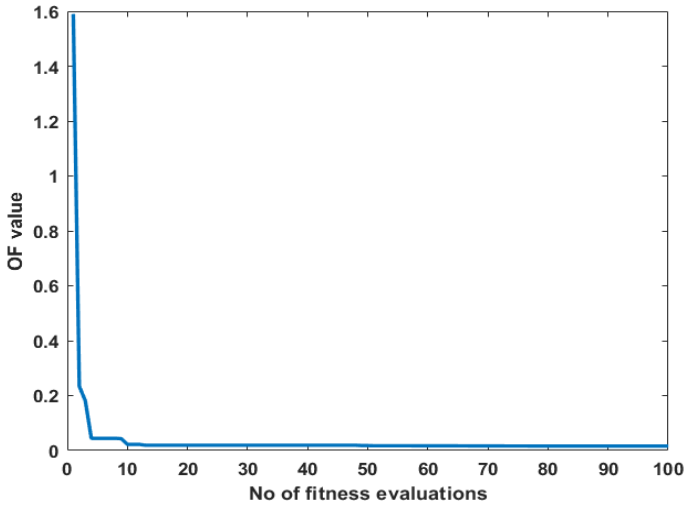

Fig. 7. Resulting convergence of the optimization's objectv\ive function..

Fig. 7 shows the performance of MVMO. The algorithm is able to effectively minimize the value of the proposed OF without the need of too many iterations. This significantly reduces the computational burden and produces high-quality results in terms of the frequency response..

6. Concluding Reflections

The chapter presents a multi-area multi-energy HVDC-HVAC cyber-physical power system and an optimization problem statement for optimal calibration of the parameters of FFC attached to PEI elements. The system can be configured and is suitable for studying different penetration levels of PEI, which is essential for the design of new HVDC-HVDC architectures. Such investigations unlock the potential of new technological upgrades for accelerated energy transition towards 100% stable and affordable sustainable and highly integrated energy systems

The developed case study attempts to illustrate the implications of creating an artificially coupled fast active power - frequency support within the context of a PEI-isolated (i.e., electromagnetically decoupled) multi-area multi energy HVDC-HVAC systems. Numerical analysis conducted by using DPF2022 show that active power imbalances can be optimally and effectively tackled by the PEI elements equipped with FFC, which are deployed in the affected synchronous area, and with the support of PEIs with FFC like those attached to VSC-HVDC inter-area links and the PEIs with FFC from other synchronous areas. The proposed optimization problem statement allows defining FFS by other PEIs as a function of the available kinetic energy and active power headrooms, without altering the intra-area active power balances of the external synchronous areas. Hence, by using the proposed optimization problem statement, it is possible to target a preservation of the time evolution of the dynamic frequency response in the involved synchronous areas in line with the operational limits pursued by a TSO. A powerful optimization solver is needed to tackle the optimization of FFCs of PEI within limited computing budget. The MVMO seems an attractive option as shown in this chapter. Future research will cover the study of other HVDC-HVAC architectures and optimization solvers.

References

[1] A. Halley, N. Martins, P. Gomes, D. Jacobson, W. Sattinger, Y. Fang, L. Haarla, Z. Emin, M. Val Escudero, S. Almeida De Graaff, V. Sewdien and A. Bose: "Effects of increasing power electronics-based technology on power system stability: Performance and operations", CIGRE Science & Engineering, vol. 11, pp. 5-17, June 2018.

[2] A. Khan, M. Hosseinzadehtaher, M. B. Shadmand, S. Bayhan and H. Abu-Rub, " On the Stability of the Power Electronics-Dominated Grid: A New Energy Paradigm," in IEEE Industrial Electronics Magazine, vol.14,no.4,pp.65-78, Dec. 2020, doi: 10.1109/MIE.2020.3002523.

[3] Yuan, X., Hu, J. & Cheng, S."Multi-time scale dynamics in power electronics-dominated power systems," Front. Mech. Eng. 12, 303–311 (2017). https://doi.org/10.1007/s11465-017-0428-z.

[4] N. Hatziargyriou, J. V. Milanović, C. Rahmann, V. Ajjarapu, C. Cañizares, I. Erlich, D. Hill, I. Hiskens, I. Kamwa, B. Pal, P. Pourbeik, J. J. Sanchez-Gasca, A. Stanković, T. Van Cutsem, V. Vittal and C. Vournas: "Definition and Classification of Power System Stability – Revised and Extended", IEEE Transactions on Power Systems, December 2020.

[5] L. Meegahapola, A. Sguarezi, J.S. Bryant, M. Gu, D. E. R.Conde R. B. A. Cunha. "Power System Stability with Power-Electronic Converter Interfaced Renewable Power Generation: Present Issues and Future Trends",Energies 2020, 13,3441. https://doi.org/10.3390/en13133441.

[6] V.N. Sewdien, R. Chatterjee, M. Val Escudero, and J. Van Putten,"System Operational Challenges from the Energy Transition," CIGRE Science & Engineering, vol.17, pp. 5-19, Feb. 2020.

[7] P Maibach, A. Hernandez, J. Peiro, C. Smith, V. Sewdien and J. van Putten, " Capabilities of Power Electronic Devices in Enabling the Energy Transition and Mitigating System Operational Challenges," CIGRE Science & Engineering, vol.20, pp. 125-136, Feb. 2021.

[8] E. Rakhshani, A. Perilla, J. L. R. Torres, F. M. Gonzalez-Longatt, T. B. Soeiro and M. A. M. M. Van Der Meijden, "FAPI Controller for Frequency Support in Low-Inertia Power Systems," in IEEE Open Access Journal of Power and Energy, vol. 7, pp. 276-286, 2020, doi: 10.1109/OAJPE.2020.3010224.

[9] Crăciun, B., Kerekes T., Séra D., Teodorescu R., and Annakkage U., Power ramp limitation capabilities of large PV power plants with active power reserves. IEEE Transactions on Sustainable Energy, vol. 8, no. 2, pp. 573–581, 2017.

[10] Karaolanis, A., Perilla A., Rueda, J.L., van der Meijden M., and Alefragkis A., Generic model of a VSC-based HVDC link for RMS simulations in PSS/E. IFAC-PapersOnLine, vol. 51, no. 28, pp. 303 – 308, 10th IFAC Symposium on Control of Power and Energy Systems CPES, 2018.

[11] N. Veerakumar, Z. Ahmad, M. Ebrahim Adabi, J. L. Rueda Torres, P. Palensky, M.A.M.M. van der Meijden, F. Gonzalez-Longatt, "Fast Active Power - Frequency Support Methods in Large Scale Electrolyzers for Multi-Energy Systems", in 2020 IEEE PES Innovative Smart Grid Technologies Europe (ISGT-Europe), The Hague, The Netherlands, October 2020.

[12] A.D. Perilla Guerra, J. L. Rueda Torres, A.A. van der Meer, M.A.M.M. van den Meijden and A. Alefragkis, "Influence of Active Power Gradient Control of an MMC-HVDC Link on Long-Term Frequency Stability", in 2017 IEEE Power & Energy Society General Meeting, Chicago, IL, USA 2017.

[13] A.D. Perilla Guerra, D. Gusain, J.L. Rueda Torres, P. Palensky, M.A.M.M. van der Meijden, F. Gonzalez-Longatt, "Optimal Tuning of Active Power Control for Frequency Support in Multi-Energy Systems", in 2020 IEEE PES Innovative Smart Grid Technologies Europe (ISGT-Europe), The Hague, The Netherlands, October 2020.

[14] J.L. Rueda Torres, A.D. Perilla Guerra, E. Rakhshani, P. Palensky, M.A.M.M. van der Meijden and A. Alefragkis, "MVMO-based Tuning of Active Power Gradient Control of VSC-HVDC Links for Frequency Support", in 2019 2nd International Conference on Smart Grid and Renewable Energy(SGRE), Doha, Qatar, 2019.

[15] F. M. Gonzalez-Longatt and J. L. Rueda Torres, "PowerFactory Applications for Power System Analysis", Springer, Delft, The Netherlands, 2014.

[16] Hydrogen Council, "Hydrogen Scaling up – A Sustainable Pathway for the Global Energy Transition", Hydrogen Council Tech. Rep., Nov. 2017.

[17] DIgSILENT GmbH, "PowerFactory Seminar HVDC and Facts", DIgSILENT GmbH, Tech. Rep., June 2018, Gomaringen, Germany.

[18] CIGRE Working Group B4.57, "Guide for the Development of Models for HVDC Converters in a HVDC Grid", CIGRE, Tech. Rep., December 2014.

[19] N. T. Trinh, M. Zeller, K. Wuerflinger, and I. Erlich, "Generic Model of MMC-VSC-HVDC for Interaction Study With AC Power System," IEEE Transactions on Power Systems, vol.31, no.1, pp.27-34, Jan. 2016.

[20] "Stability Analysis of an International Electricity System Connected to Regional Local Sustainable Gas Systems", TSO 2020 Activity 2 Final Report, 2019.

[21] P. Kundur, " Power System Stability and Control", McGraw-Hill Professional, 1st Edition, 1994.

[22] Wang, W., Beddard, A., Barnes M., and Marjanovic O., Analysis of active power control for VSC HVDC, IEEE Transactions on Power Delivery, vol. 29, no. 4, pp. 1978–1988, 2014.

[23] B. W. Tuinema, E. Adabi, P.K.S. Ayivor, V. Garcia Suarez, L. Liu, A.D. Perilla Guerra, Z. Ahmad, J. L. Rueda Torres, M.A.M.M. van der Meijden, P.Palensky, "Modelling of Large-sized Electrolysers for Real-Time Simulation and Study of the Possibility of Frequency Support by Electrolysers", IET Generation, Transmission & Distribution, vol.14, no.10, pp. 1985-1992, 13 May 2020.

[24] P. Ayivor, J. L. Rueda Torres, M.A.M.M. van der Meijden, R. van der Pluijm and B. Stouwie, " Modelling of Large Size Electrolyzer for Electrical Grid Stability Studies in Real Time Digital Simulation", in Proc. of Energynautics 3rd International Hybrid Power Systems Workshop, Tenerife, Spain, May 2018.

[25] G.Giannakopoulos, "Master Thesis: Optimal Tuning of the Active Power Gradient Control in Multi-Energy HVDC-HVAC Power Systems", Delft University of Technonolgy, April 2021, Delft, Netherlands.

[26] J. L. Rueda Torres and I. Erlich, " Hybrid Single Parent-Offspring MVMO for Solving CEC2018 Computationally Expensive Problems", 2018 IEEE World Congress on Computational Intelligence, pp. 1-8, Rio de Janeiro Brazil, July 2018.

[27] European Commission, "Commission Regulation (EU) 2017/1485 of 2 August 2017 establishing a guideline on electricity transmission system operation", European Commission, Brussels 2017.